PERMEABILITY CHANGE UNDER DIFFERENT STRESS AND FLUID PRESSURE CONDITIONS

Russ Ewy, Paul Hagin, Craig Bovberg and Mark Shalz
Chevron Energy Technology Co., San Ramon, CA and Richmond, CA, USA

ABSTRACT

Permeability is commonly assumed to be a function of effective stress (the difference between stress and fluid pressure). This approach allows permeability to be measured with very low values of fluid pressure in the laboratory. To test if this is valid, we developed a system to measure permeability along the axis of a rock sample, for which axial stress, confining stress, and fluid pressure can all be varied independently, and with fluid pressures approaching 138 MPa (20,000 psi). We present results from several consolidated reservoir sandstones, showing that the effective stress coefficient for permeability is less than one over a large range of stress and pressure conditions, but that it can exceed one at low effective stress. However, the effective stress coefficient alone does not allow prediction of the depletion response, which requires direct measurement. In these tests, the highest stress is orthogonal to flow, to duplicate conditions that are important for reservoir production. The results compare favorably with those obtained under true uniaxial-strain conditions, but both are different from those obtained under hydrostatic conditions. Our method generates permeability vs. depletion results that are more applicable to field conditions than those from standard hydrostatic tests.

INTRODUCTION

For most reservoirs, the most important permeability to measure is the horizontal permeability. However, the vertical stress is usually greater than the horizontal stress, and this stress difference could impact the permeability. Furthermore, as the reservoir pressure declines due to production, the 'effective' vertical stress (vertical stress minus fluid pressure) increases, and this reduces the formation permeability in the horizontal direction. Thus, it is important to measure the horizontal permeability under conditions of realistic vertical and horizontal stress, and also to quantify the change in permeability due to a reduction in the fluid pressure.

Permeability is commonly measured assuming the 'effective stress law', which considers only the difference between stress and fluid pressure. This approach allows permeability to be measured with very low values of fluid pressure in the laboratory, simulating depletion by increasing stress with constant low fluid pressure. However, it is likely that

permeability at high stress and high fluid pressure will be different than permeability at low stress and low fluid pressure, even for the same 'effective stress' (stress minus fluid pressure). This is because the pore pressure may influence the permeability differently than confining stress. Although not an exhaustive list, laboratory measurements that show this effect can be found in [1-7]. Some researchers report pore pressure having less effect than confining stress [e.g. 2, 6], some report it having more effect [e.g. 1, 4, 5, 7], and some found both types of behavior [e.g. 3].

We have developed a system to measure permeability along the axis of a cylindrical rock sample, for which axial stress, confining stress, and fluid pressure can all be varied independently. Furthermore, it can successfully measure permeability at fluid pressures approaching 138 MPa (20,000 psi). By applying axial stress less than confining stress, and using samples with their axis parallel to horizontal bedding, horizontal permeability under realistic *in situ* stress conditions is easily obtainable. An advantage of this method is that the flow path is one-dimensional.

APPARATUS
A concept that we have used with two different systems is to flow along the sample axis but maintain axial stress less than confining stress. The axial stress represents the minimum horizontal stress, while the confining stress represents the vertical stress and the maximum horizontal stress. Samples are cut with their axes parallel to horizontal bedding. Using this approach, the horizontal permeability is measured under stress conditions which are similar to *in situ* conditions, certainly more so than equal stress in all directions. Because flow is one-dimensional, steady-state flow is easily achieved and verified, and industry-standard methods for permeability interpretation can be used.

Our first method of employing this technique is referred to as the "low pressure" apparatus, and also as the "biaxial stress" method. We adapted a standard 'Hassler' cell so that a piston, rather than just high-pressure tubing, could pass through the end of the cell. The piston has a small-diameter bore down the middle, to provide fluid access to the sample pore space. The part of the piston that passes through the seals has a diameter smaller than the sample diameter (diagram in Ref 8). The amount of axial force on the sample is determined by the annular area that is acted upon axially by the confining fluid. We have machined pistons to provide confining:axial stress ratios equal to 2.0, 2.78 and 3.5, but any ratio is achievable.

A variable ratio of confining to axial stress is more versatile than a fixed ratio, so our most recent apparatus includes this capability. In the new apparatus (referred to as the "high pressure" apparatus), axial stress and confining stress are completely independent. A schematic of this apparatus is shown in Figure 1. Axial stress is provided by pressurized fluid inside a self-contained chamber at one end of the apparatus, which drives the piston. The axial stress can be less than or greater than the confining stress.

The pressure limits of the apparatus are 138 MPa for the confining stress, axial stress, and pore pressure (138 MPa = 20,000 psi). Flow is achieved by flowing from one high-pressure pump to another high-pressure pump [8]. Axial stress is determined from the applied fluid pressure and is verified using a load cell positioned inside the apparatus (not shown). The apparatus also contains electronic feedthroughs so that strain-measuring devices (LVDT's or other methods) can be installed on the sample.
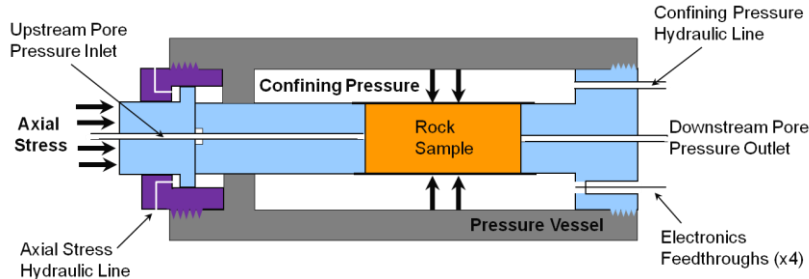
Figure 1. Schematic of apparatus for obtaining any independent values of confining stress, axial stress, and pore pressure. For constant stress ratio apparatus, see [8].

METHODOLOGY

Test Procedure

The main goal of the tests is to measure permeability reduction due to reservoir pressure depletion. When reservoir pressure declines, most reservoir formations deform in the vertical direction but deform very little in the horizontal direction ('uniaxial-strain'). Associated with this is a decline in the total horizontal stress (the 'stress path'). We approximate this effect by using the axial stress to represent the horizontal stress, based on stress paths measured in uniaxial-strain tests. For tests using the machined piston (and constant low pore pressure), an appropriate constant stress ratio is chosen that provides effective stresses similar to the initial values in the reservoir and also closely follows the expected stress path due to depletion. For the device in Figure 1, the actual *in situ* values of vertical stress, horizontal stress and pore pressure can be duplicated quite closely, both for initial conditions and for horizontal stress change due to depletion.

Stress and/or pore pressure changes are imposed in a stepwise manner to simulate depletion. This is shown graphically in Figure 2a and 2b. For tests with constant and low pore pressure, the depletion effect is simulated by increasing both the confining stress and axial stress, with the axial stress increasing by less than the confining stress. For tests with true simulated depletion (changing pore pressure), the pore pressure is stepwise reduced starting from a very high value, with the confining stress maintained constant. With each step of pore pressure reduction the axial stress is reduced by the appropriate amount to give the desired stress path. As illustrated in Figure 2, the loading is always reversed once maximum simulated depletion has been reached. This is to test

for reversibility of permeability vs. stress/pressure behavior, quantify hysteresis, and obtain true elastic behavior. Unloading response examples can be found in [8].

One potential drawback of these methods is that the effective confining stress, which represents the greatest stress in the reservoir, acts around the entire sample circumference, creating a high horizontal stress in one direction. This might be appropriate for certain areas in the near-wellbore region. However, away from the wellbore the maximum horizontal stress is expected to decrease in a manner similar to the minimum horizontal stress, if uniaxial-strain conditions prevail. This effect cannot be directly included in the tests, but the results can be corrected for stress path effects when appropriate. For example, permeability can be expressed as a function of mean effective stress on the sample rather than effective confining stress, and this can be directly related to mean effective stress in the reservoir. An example is shown later in the paper.
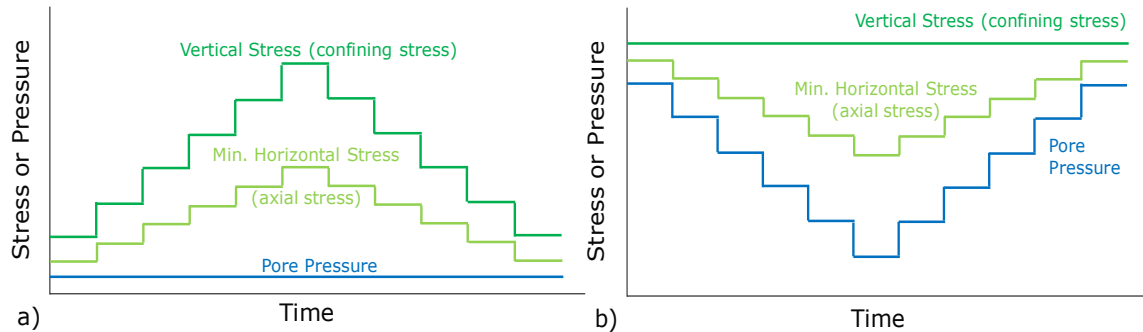
Figure 2. Stepwise changes in stress and/or pressure to simulate depletion and reverse depletion, using two different approaches: a) changing stress with constant low pore pressure, b) actual pore pressure depletion.

Permeability Calculation

At each stress/pressure step, four different flow rates are imposed on the sample. For each flow rate an equilibrium (steady-state) pressure drop is measured. A best-fit slope is determined from the four data pairs ($Q*\mu$, ΔP) resulting from the four different flow rates, where Q is volumetric flow rate, μ is fluid viscosity and ΔP is pressure drop. Because permeability is proportional to the term ($Q*\mu/\Delta P$) which is the slope of the linear fit, permeability (k) is then easily calculated using the equation

$$k = (Q*\mu/\Delta P)*(L/A) \qquad\qquad (1)$$

where L is sample length and A is cross-sectional area, and the slope is substituted for the term ($Q*\mu/\Delta P$). If the four data points do not form a straight line but are bi-linear or curved, then a fit to the first three or last three data points is used instead, if it provides a better correlation coefficient. As a quality control check, permeability is also calculated separately for each flow rate, and this is done in two different ways (details in Ref. 8).

In order to accurately determine permeability, we had to characterize the fluid viscosity as a function of both pressure and temperature, up to very high pressure values. We used two different methods, 1) capillary tube and 2) electromagnetic viscometer (EMV). Viscosity of the Paratherm NF® fluid (Paratherm Corporation) was measured using each device, at three different temperatures and from very low pressure up to very high pressure. Further details can be found in [8]. When using oil, permeability at low fluid pressure is most impacted by the temperature correction while at high (and changing) fluid pressure it is most impacted by the viscosity vs. pressure relationship.

RESULTS

Sample Description and Test Protocol

A series of tests was performed on core samples from a deep sandstone reservoir. The great depth, and high overpressure, of this reservoir necessitated testing at very high values of stress and pressure in order to duplicate *in situ* conditions. For comparison, tests were performed using low values of fluid pressure. The samples tested are listed in Table 1. Eight of the samples form two groups of four samples each, based on porosity and permeability. Two additional samples (dSU samples) also belong to Group 1.

Table 1. Samples used for testing. Porosity and air permeability are measured under ~3 MPa net stress, after sample cleaning. Air permeability is measured at the exact sample depth, except for dP2d.

Sample	Forma-tion	Porosity (%)	Air Perm (md)	Sample	Forma-tion	Porosity (%)	Air Perm (md)
Group 1	**1**	**~20**	**15 – 25**	**Group 2**	**2**	**~22.5**	**25 – 35**
dS1a	1	19.8	23.5	dS2a	2	22.1	28.3
dS1b	1	20.6	20.0	dS2b	2	22.7	22.6
dP1c	1	19.5	16.9	dP2c	2	22.2	28.7
dP1d	1	19.5	19.4	dP2d	2	22.6	~37
dSU1e	1	20.4	24.0				
dSU1f	1	19.3	21.0				

The sequences of stress and pressure applied to the samples are shown generically in Figure 2. Samples labeled dS were tested by increasing (then decreasing) the stresses with a constant pore pressure of ~0.7 MPa. Confining stress was increased from 22.7 MPa to 119 MPa, with the axial stress equal to 0.36 times the confining stress (a machined piston was used for these tests). Samples labeled dP were tested by decreasing (then increasing) the pore pressure from 114 MPa to 16 MPa with a constant confining stress of 134.5 MPa and a starting axial stress of 122 MPa. The axial stress was reduced by ~0.69 times the pore pressure reduction, for each step. These tests were performed using the device illustrated in Figure 1. The dSU samples were tested under uniaxial-strain conditions and are discussed in a later section.

The stress and/or pressure changes were applied in a stepwise fashion, as illustrated in Figure 2. Each step (typically 14-20 MPa change in effective confining stress) lasted roughly 330 to 350 minutes of hold time. This consisted of a wait at zero flow rate (for stress response) followed by sufficient time at each of the four flow rates to obtain steady-state data. Unloading results can be found in [8].

Delta-Stress vs. Delta-Pressure Results

We found that permeability measurements performed by changing stress rather than pore pressure may not correctly predict how permeability will evolve in a reservoir as fluid pressure changes. Results for Group 2 samples are shown in Figure 3 for the loading phase (increasing effective stress, whether through stress increase or through pore pressure decrease). Permeability is plotted as a function of the difference between the confining stress and pore pressure. Permeability values are normalized because each sample has a slightly different overall magnitude of permeability. They are normalized to the permeability measured at maximum effective stress. The states are not exactly the same, as the values of stress and pressure are about 15 MPa greater for the dP tests compared to the dS tests. However, this state of high stress and low fluid pressure is the point during all tests where the stress and pressure states are the most similar.
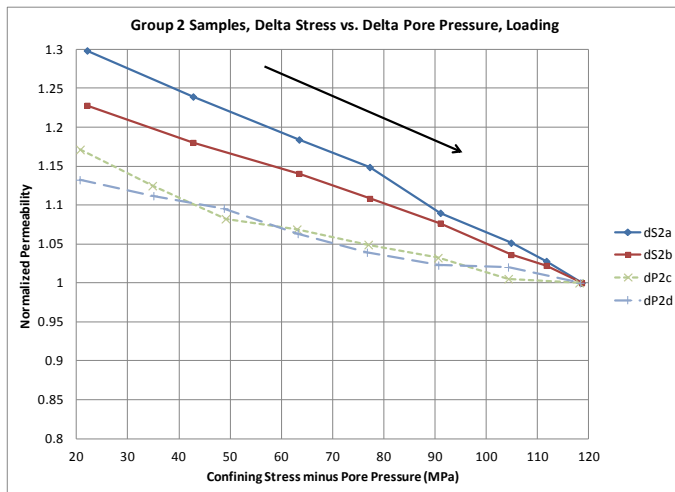
Figure 3. Permeability due to increasing stress (dS) or decreasing pore pressure (dP), for Group 2 samples.

The influence of stress and pore pressure on permeability can be expressed by the equation

$$k = f(P_c - n_k P_p) \qquad (2)$$

where k is permeability (or normalized permeability), P_p is pore pressure and P_c is confining stress. n_k is the effective stress coefficient for permeability. If n_k is close to 1 then a change in stress will alter permeability by the same amount as an equal and opposite change in pore pressure. In this paper, n_k is treated as an empirical parameter

which is unrelated to α, the Biot coefficient which describes changes in rock bulk volume.

Figure 4a illustrates the loading paths imposed on the dS and dP samples, along with a constant effective stress approach (dPS). The dS and dP tests are two different ways of crossing values of effective stress (shown by the dashed gray lines). If $n_k=1$, then lines of constant permeability (iso-permeability lines) will be exactly parallel to these lines of constant effective stress. An approximate interpretation of the results in Figure 3 is shown in Figure 4b, replacing the effective stress lines with the observed iso-permeability lines. The lines have a slope less than 1, indicating that $n_k<1$ at both low and high effective stress. Note that the iso-permeability lines may not be straight as illustrated; however, we have little information other than that obtained from the dS and dP paths.
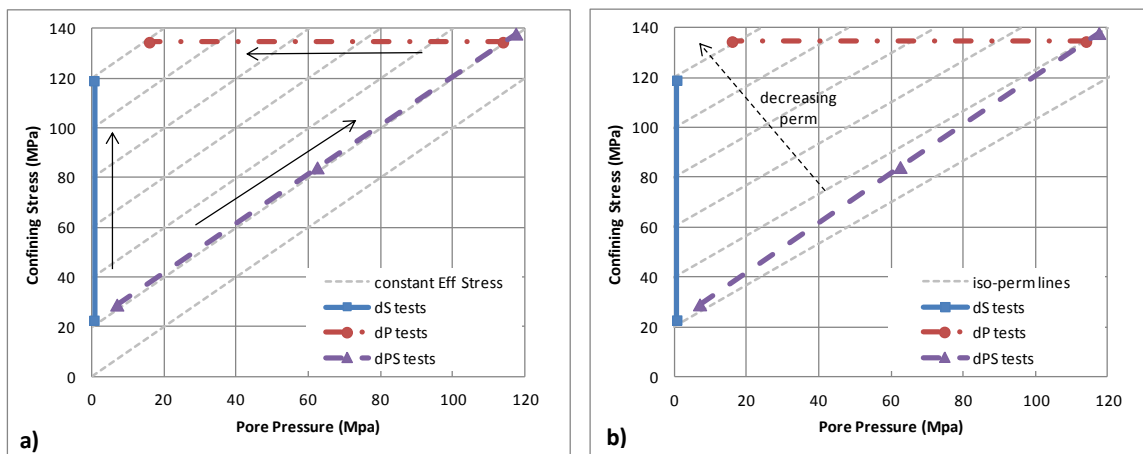
Figure 4. a) Values of changing stress and/or pore pressure applied in the dP, dS and dPS (constant effective stress) tests. Dashed gray lines are lines of constant effective stress. b) illustrative interpretation of response observed in Figure 3; iso-permeability lines have a slope less than one.

A different behavior was observed on the Group 1 samples, shown in Figure 5. Both the dS and the dP tests show non-linear change of permeability due to increasing effective stress, but the dP tests are much more non-linear (more curved). Moreover, at low effective stress the dP tests result in a larger change in permeability than the dS tests. This suggests $n_k>1$. At high effective stress there is less change in permeability in the dP tests, compared to the dS tests, which corresponds to $n_k<1$.
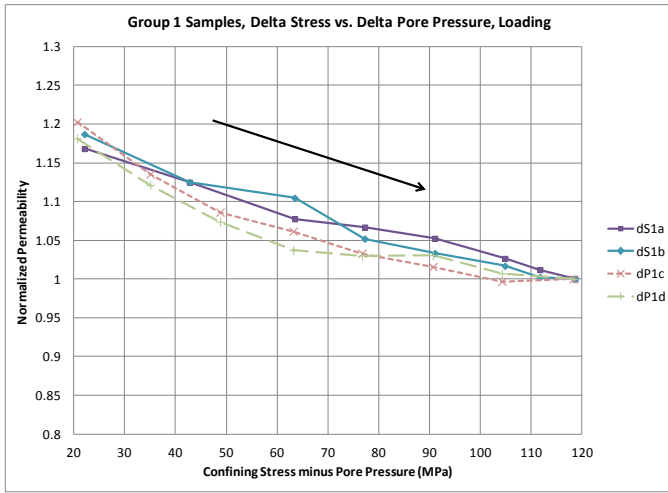
Figure 5. Permeability due to increasing stress (dS) or decreasing pore pressure (dP), for Group 1 samples.

Figure 6 shows idealized interpretations of the Group 1 response, modeling a linear dS behavior combined with a non-linear dP behavior. Along the dP path, at low fluid pressure the iso-permeability lines are spread out and have a slope less than 1, while at high fluid pressure the lines are close together and have a slope greater than 1. Assuming straight iso-permeability lines, this behavior corresponds to $n_k<1$ at high effective stress and $n_k>1$ at low effective stress. Figure 6 illustrates an approximation in Figure 5 that is actually in error. The permeability at the highest effective stress for the two tests cannot be assumed to be the same, even though the stress states are similar. A more accurate analysis would require extrapolation of the measured permeability values to the point where the two tests have exactly the same values of stress and fluid pressure.
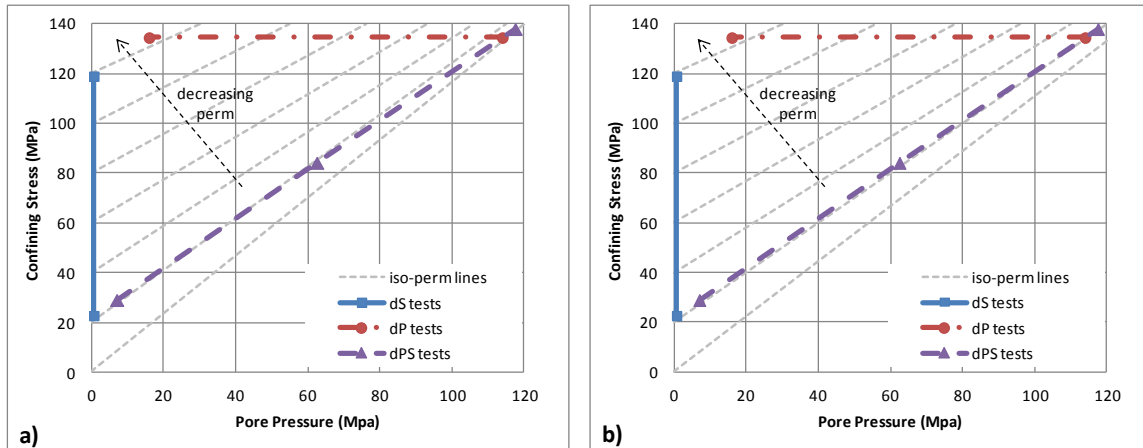
Figure 6. Two similar, but slightly different, idealized interpretations of the Group 1 results. Both illustrate $n_k>1$ at low effective stress and $n_k<1$ at high effective stress. Note the effect on the dPS path.

Other researchers have also reported the effective stress coefficient for permeability to be less than one [e.g. 2, 3, 6], and some have also reported it to not be constant [3, 6]. When it was found to not be constant [3, 6], it was always lowest for the situation of high stress combined with low pore pressure; raising the pore pressure, or reducing the stress, caused the effective stress coefficient to increase in value (see Fig. 11 Ref. 3, Fig. 6 Ref. 6). Li et al [6] report extremely low values of the effective stress coefficient for the combination of high confining stress and low pore pressure; this also agrees well with our findings. Effective stress coefficient values greater than one are also reported in the literature [e.g. 1, 3, 4, 5, 7]. We too find this, although only at low effective stress.

The physical mechanism explaining $n_k<1$ is similar to the mechanism explaining Biot's coefficient (α) being less than one. The pore volume is influenced less by pore pressure than it is by confining stress. The physical mechanism explaining $n_k>1$ is usually associated with pore linings or grain coatings that are compressed more by pore pressure than they are by confining stress [1, 9]. Interestingly, our observation that n_k decreases with increasing effective stress is in line with α empirically decreasing with increasing stress (due to decreasing rock frame compressibility).

The dPS (constant effective stress) path was applied to four samples, three of which are described and analyzed in [8]. These three samples generated mixed results, some indicating increasing permeability due to simultaneous increase of stress and pressure (e.g. Figure 6a) and some indicating decreasing permeability (e.g. Figure 4b). The fourth sample is a more recent test on a sample with 24% porosity and ~80 md air permeability. For this sample, permeability was measured at each of the three triangle positions indicated in Figure 4a. Interpretation using the capillary-tube-determined viscosity indicates permeability 1.4% greater at the second measurement point (compared to the first) and 6.8% greater at the final measurement point (compared to the first). This corresponds to the behavior illustrated in Figure 6a. However, interpretation using the EMV-determined viscosity indicates constant permeability at all three measurement points (consistent with Figure 6b). These different interpretations will in turn impact the computation of the effective stress coefficient for permeability (see equations in [8]).

Note, however, that Figures 6a and 6b are only subtly different, and both are fully compatible with the behavior in Figure 5. It is possible to measure n_k by simultaneously changing stress and pore pressure by equal amounts. However, there are two drawbacks: 1) interpretation requires extremely accurate knowledge of fluid viscosity vs. pressure, and 2) the measured n_k cannot predict what will happen due to changing pore pressure at high stress / high pressure vs. changing stress at low stress / low pressure. Figures 6a and 6b both demonstrate large reduction in permeability due to changing pore pressure at high stress / high pressure. This behavior can only be measured by performing the simulated depletion (dP) test; the dPS test does not reveal it. Importantly, knowledge of n_k does not reveal the magnitude of permeability reduction due to a unit change in pore

pressure or due to a unit change in stress. Pore pressure, or stress, must be changed at the point of interest, in order to measure that effect. Measurements performed at low stress and low fluid pressure can provide misleading results, whether or not they are performed as delta-stress tests or as delta-fluid-pressure tests.

Comparison to Uniaxial-Strain and Hydrostatic Tests

Measurements of permeability vs. stress, with constant low pore pressure, were also measured on samples subjected to true uniaxial-strain boundary conditions. These were measurements of horizontal permeability across the diameter of vertical samples, performed at a vendor lab under Chevron direction using odorless mineral spirits. Sample characteristics are listed in Table 1. Results are compared to those obtained with the 'biaxial stress' approach (dS samples in Table 1) in Figure 7. The x-axis is the effective confining stress for the biaxial stress tests and it is the effective axial stress for the uniaxial-strain tests. In both cases the flow is perpendicular to the maximum stress and parallel to the least stress, and is aligned with the horizontal core direction.

It is seen that the biaxial stress tests (dS tests) result in greater permeability reduction than the uniaxial-strain tests. The most likely explanation is that the intermediate stress (which also acts perpendicular to flow) is equal to the maximum stress in the biaxial stress tests but is equal to the minimum stress in the uniaxial-strain tests. This higher intermediate stress causes further permeability reduction, for this particular sample set.

The same data are plotted against mean effective stress (average of the three stresses, minus pore pressure) in Figure 8. For this particular set of samples, it is seen that mean effective stress provides a way to relate the results obtained with the two different test conditions. This is encouraging, because we expect that deformation in the reservoir will be close to uniaxial-strain conditions. This means we can use the results of our dS tests (or preferably, our dP tests) to predict permeability reduction in the reservoir, by calculating expected changes in mean effective stress in the reservoir and relating those changes directly to our measurements.
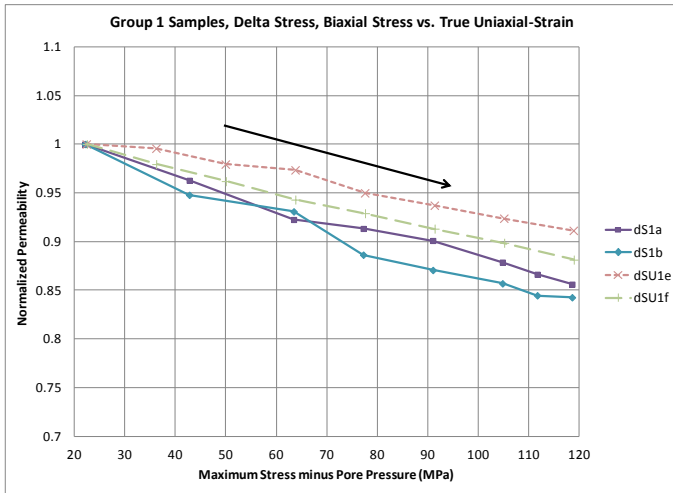
Figure 7. Horizontal permeability due to increasing stress, using biaxial stress method (dS) and uniaxial-strain on vertical samples (dSU).
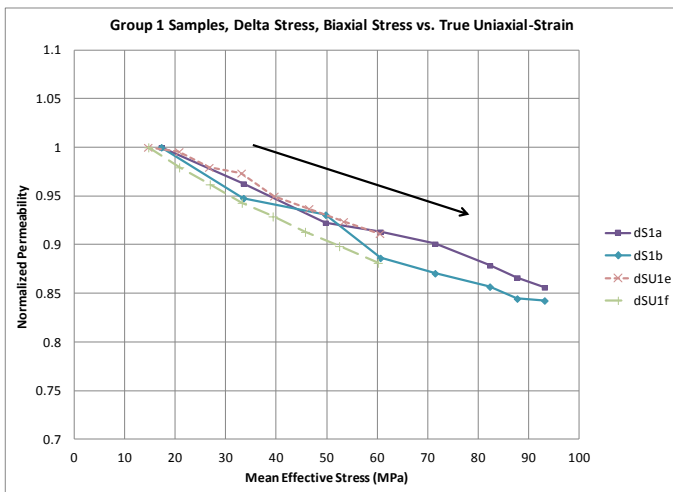
Figure 8. Same data as in Figure 7, plotted against mean effective stress.

However, even if permeability reduction can be related to the change in mean effective stress, this does not mean that it can be accurately measured using hydrostatic (equal in all directions) stress. For example, Figure 9 shows liquid permeability vs. increasing stress measured on a high-porosity weak sand, using three methods: biaxial stress (dS tests), uniaxial-strain tests, and hydrostatic tests. When plotted vs. mean effective stress, the biaxial stress test gives a permeability reduction similar to that measured in the uniaxial-strain tests, perhaps slightly greater. However, the hydrostatic tests show much less permeability reduction than the other two test approaches.

We surmise that the existence of a stress difference (vertical stress greater than horizontal stress) in reservoirs, and the fact that this stress difference increases with increasing depletion, is an important control on permeability. This stress difference is likely to result in changes in pore throats and other flow pathways that are significantly different than changes that occur with equal stresses in all directions. It is for this reason that we developed our methods (e.g. Figure 1) to measure horizontal permeability with flow parallel to the least stress and perpendicular to the greatest stress.
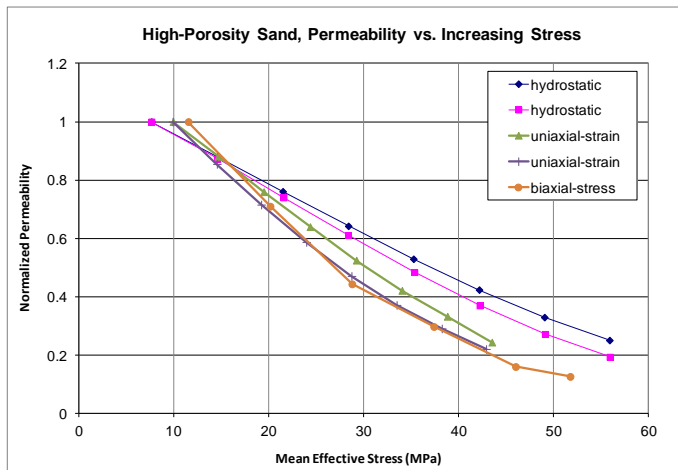
Figure 9. Permeability vs. increasing mean effective stress on a weak high-porosity sand, comparing biaxial-stress, uniaxial-strain and hydrostatic (three equal stresses).

CONCLUSIONS

We developed a system with fully-independent axial stress, confining stress and pore pressure, and the ability to measure permeability at fluid pressures approaching 138 MPa. The apparatus uses one-dimensional flow along the sample axis, parallel to the least stress. These features allow us to better simulate *in situ* conditions, including the effects of pressure depletion. By comparing the permeability response to changing stress (with constant low fluid pressure) and changing fluid pressure (with constant high stress), we found the effective stress coefficient for permeability to be less than or equal to one over a large range of stress and pressure conditions; however we also found it can be greater than one at low effective stress, and this was partially confirmed with 'constant effective stress' tests performed at low effective stress.

Because the effective stress coefficient was found to be both 1) different than one and 2) not constant, this suggests that the only accurate way to predict permeability change in a reservoir due to depletion is to perform an actual depletion test, starting at high fluid pressure (similar to reservoir conditions) and then decreasing the fluid pressure. We also conclude that measurement of the effective stress coefficient, while interesting, is not sufficient to allow prediction of the permeability vs. depletion response nor to allow 'correction' of permeability response obtained at low stress and low fluid pressure.

Permeability change using confining pressure greater than axial stress (and flow parallel to axial stress) compares well on a mean effective stress basis with that measured under true uniaxial-strain conditions. However, tests using equal stress in all directions are not expected to give the same result and may be difficult to apply to field conditions.

ACKNOWLEDGEMENTS

REFERENCES

1. Zoback, M.D and J.D. Byerlee. Permeability and effective stress. *Amer. Assoc. Pet. Geol. Bull.* (1975) 59: 154-158.
2. David, C. and M. Darot. Permeability and conductivity of sandstones. In *Proceedings of the ISRM/SPE International Symp. "Rock at Great Depth", Pau, 28-31 August 1989*, eds. V. Maury & D. Fourmaintraux, 203-209. Rotterdam: Balkema.
3. Warpinski, N.R. and L.W. Teufel. Determination of the effective stress law for permeability and deformation in low-permeability rocks. *SPE Formation Evaluation* (1992) June: 123-131.
4. Shafer, J.L., G.N. Boitnott and R.T. Ewy. Effective stress laws for petrophysical rock properties. *SPWLA 49th Annual Logging Symposium, Edinburgh, 25-28 May 2008*.
5. Boitnott, G., T. Miller and J Shafer. Pore pressure effects and permeability: Effective stress issues for high pressure reservoirs. *Int. Symp. of the Society of Core Analysts, Noordwijk aan Zee, Netherlands, 27-30 September 2009.*
6. Li, M., Y. Bernabe, W.-I. Xiao, Z.-Y. Chen and Z.-Q. Liu. Effective pressure law for permeability of E-bei sandstones. *J. Geophysical Research.* (2009) 114, B07205.
7. Ghabezloo, S., J. Sulem, S. Guedon and F. Martineau. Effective stress law for the permeability of a limestone. *Int. J. Rock Mech. & Min. Sci.* (2009) 46: 297-306.
8. Ewy, R., C. Bovberg, P. Hagin and M. Shalz. Permeability measurement with ultra-high fluid pressure and unequal stresses. Paper ARMA 12-656, *46th US Rock Mechanics / Geomechanics Symp., Chicago, 24-27 June 2012.*
9. Al-Wardy, W. and R. Zimmerman. Effective stress law for the permeability of clay-rich sandstones. *J. Geophysical Research.* (2004) 109, B04203.